GROUND DATA PROCESSING & PRODUCTION OF THE LEVEL 1 HIGH RESOLUTION MAPS

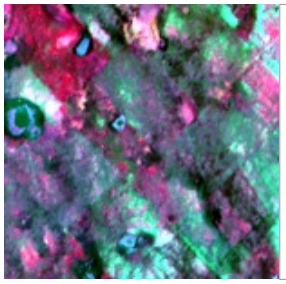

VALERI 2002

Laprida site
(grassland)

Philippe Rossello, Marie Weiss

December 2005

CONTENTS

1. Introduction **2**
2. Available data **2**
2.1. SPOT Image 2
2.2. Hemispherical images 3
2.3. Sampling strategy 5
2.3.1. Principles 5
2.3.2. Evaluation based on NDVI values 6
2.3.3. Evaluation based on classification 7
2.3.4. Using convex hulls 9
3. Determination of the transfer function for the 6 biophysical variables: LAIeff, LAItrue, LAI57eff, LAI57true, fCover, fAPAR **10**
3.1. The transfer functions considered 10
3.2. Results 10
4. Conclusion **10**
5. Acknowledgements **11**
ANNEX **12**
Ground measurement acquisition report for the VALERI site Laprida 13

1. Introduction

This report describes the production of the high resolution, level 1, biophysical variable maps for the Laprida site in 2002 (see campaign report for more details about the site and the ground measurement campaign: annex or http://www.avignon.inra.fr/valeri). Level 1 map corresponds to the map derived from the determination of a transfer function between reflectance values of the SPOT image acquired during (or around) the ground campaign, and biophysical variable measurements (hemispherical images). For each Elementary Sampling Unit (ESU), the hemispherical images were processed using the CAN-EYE software (Version 3.5) developed at INRA-CSE. The derived biophysical variable maps are:

• four Leaf Area Index (LAI) are considered: effective LAI (LAIeff) and true LAI (LAItrue) derived from the description of the gap fraction as a function of the view zenith angle; effective LAI57 (LAI57eff) and true LAI57 (LAI57true) derived from the gap fraction at 57.5°, which is independent on the leaf inclination. Effective LAI and effective LAI57 do not take into account clumping effect. LAItrue and LAI57true are derived using the method proposed by Lang and Yueqin[1] (1986);

• cover fraction (fCover): it is the percentage of soil covered by vegetation. To improve the spatial sampling, fCover was computed over 0 to 10° zenith angle;

• fAPAR: it is the fraction of Absorbed Photosynthetically Active Radiation (PAR=400-700nm). The fAPAR is defined either instantaneously (for a given solar position) or integrated all over the day. Following a study based on radiative transfer model simulations, it has been shown that the root mean square error between instantaneous fAPAR computed every 30 minutes and the daily fAPAR is the lowest for instantaneous fAPAR at 10h00 AM (solar time, RMSE = 0.021). Therefore, the derivation of fAPAR from CAN-EYE corresponds to the instantaneous black sky fAPAR at 10h00 AM.

The land cover is composed of grasslands. The site is quite flat (altitude: ≈ 200 m). The detailed description of the site is available in the campaign report[2].

The site coordinates are described in Table 1:

	UTM 20, South WGS84 (units = meters)		Geographic Lat/Lon WGS84 (units = degrees)	
	Lat.	Lon.	Lat.	Lon.
Upper left corner	5904909	716279	-36,9770972	-60,5701777
Lower right corner	5901909	719279	-37,0034194	-60,5356305
Center	5903409	717779	-36,9902583	-60,5529041

Table 1. Description of the site coordinates.

The ground measurements were carried out from 2002/10/18 to 2002/10/19, while the high spatial resolution image (SPOT4, HRVIR2, resolution: 20 m) was acquired on 2002/11/13.

2. Available data

2.1. SPOT Image

The SPOT image was acquired the 13th November 2002 by HRVIR2 on SPOT4. It was geo-located by SPOTimage (SPOTView basic). The projection is UTM 20 South, WGS-84 (please, refer to the campaign report for more details: annex or http://www.avignon.inra.fr/valeri). No atmospheric correction was applied to the image since no atmospheric data were available. However, as the SPOT image is used to compute empirical relationships between reflectance and biophysical variable, we can assume that the effect of the atmosphere is the same over the whole 3 x 3 km site. Therefore, it will be taken into account everywhere in the same way.

Figure 1 shows the relationship between Red and near infrared (NIR) SPOT channels: the soil line is well marked and no saturated points are observed.

[1] Lang, A.R.G. and Yueqin, X., 1986. Estimation of leaf area index from transmission of direct sunlight in discontinuous canopies. Agric. For. Meteorol., 37: 229-243.
[2] Annex or http://www.avignon.inra.fr/valeri

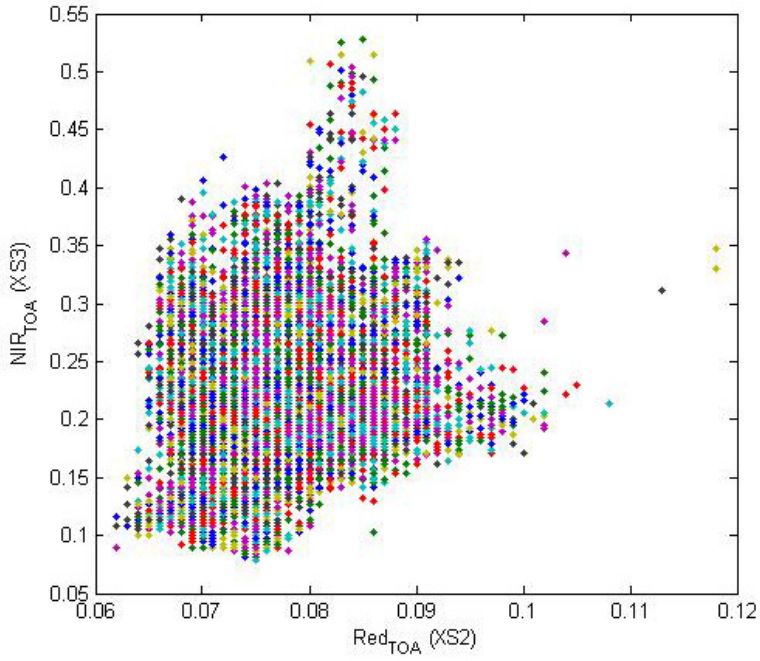

Figure 1. Red/NIR relationship on the SPOT image for Laprida, 2002.

2.2. Hemispherical images

The hemispherical images were processed using the CAN-EYE software (Version 3.5) to derive the biophysical variables. A first process was carried out with the Version 3.2. Figure 2 shows the comparison between the LAIeff results of the hemispherical images processing using two different CAN-EYE versions. The relationship is consistent, even if differences are visible. The "user effect" is probably a determinant factor.

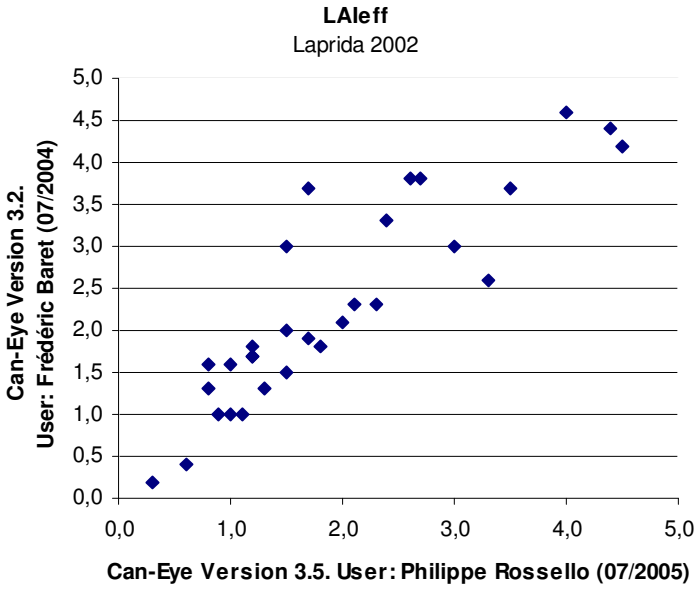

Figure 2. Comparison of CAN-EYE processing results from two versions used by different users (points in blue correspond to 30 ESUs).

Figure 3 and Figure 4 show the distribution of the several variables over the 30 sampled ESUs. As Laprida is a grassland site, all the hemispherical images were acquired from above the canopy.

Note that LAI (effective and true) derived from directional gap fraction and LAI derived from gap fraction at 57.5° (effective and true) are consistent (Figure 3 and Figure 4). Effective LAI (LAIeff, LAI57eff) varies from 0.26 to 4.5, while true LAI (LAItrue, LAI57true) varies from 0.36 to 6.75. This range shows a heterogeneous site in terms of LAI. For values, LAIeff and LAI57eff are lower than LAItrue and LAI57true. This is due to the

clumping observed for several ESUs. The relationship between fAPAR and LAI is in agreement with what is expected (Beer-Lambert law) while the fCover-LAI relationship is more noisy.

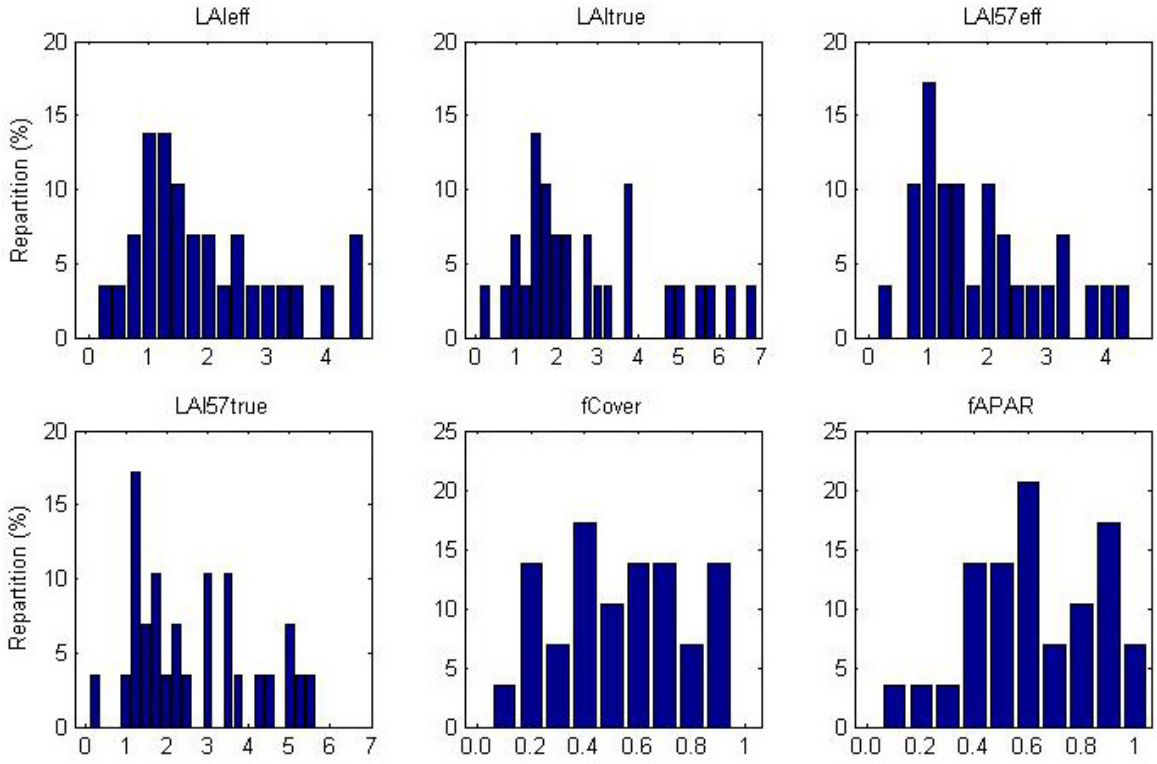

Figure 3. Distribution of the measured biophysical variables over the ESUs.

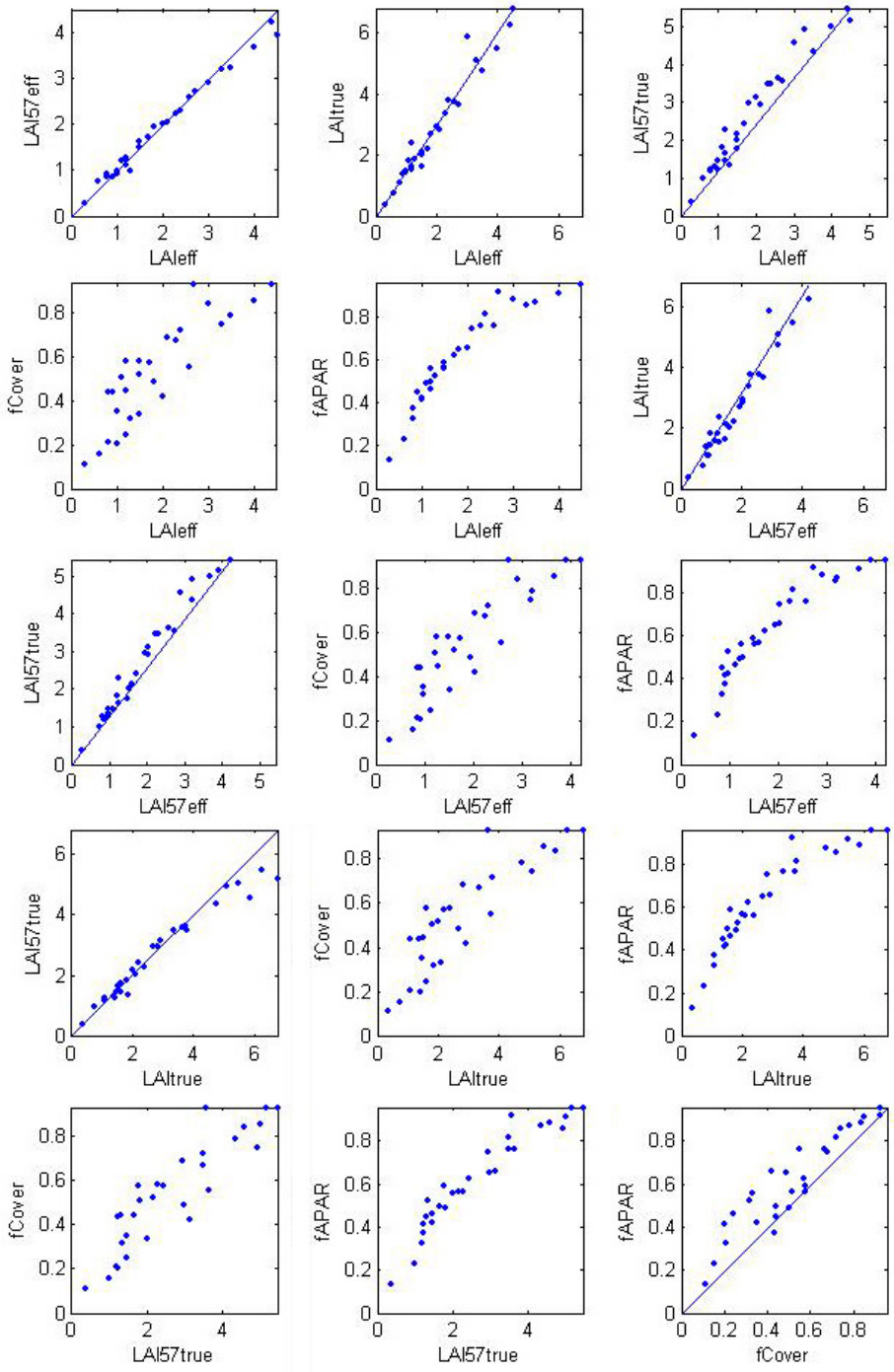

Figure 4. Relationships between the different biophysical variables

2.3. Sampling strategy

2.3.1. Principles

The sampling strategy is defined in the campaign report[3]. The sampling of each ESU is based on twelve elementary photographs organized in a cross pattern.

Figure 5 shows that the 30 ESUs are evenly distributed over the site (3 x 3 km). The processing of the ground data has shown that:

[3] Annex or http://www.avignon.inra.fr/valeri

• ESU A17 (in black on Figure 5) was located on a small plot with a strong heterogeneity on the borders. This ESU was eliminated;
• considering that SPOT geo-location and GPS measurements are associated to errors, we found that processed LAI for ESUs A11, A12, A24 and E29 did not correspond to the SPOT pixel in terms of reflectance as compared to the knowledge of the land use: they have been shifted by 1 or 2 pixels.

Finally 29 ESUs have been kept for the computation of the transfer function.

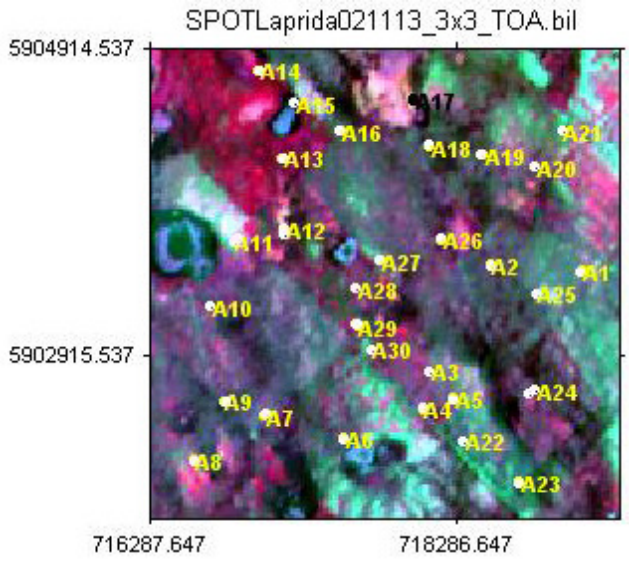

Figure 5. Distribution of the ESUs around the Larose site. ESU in black (A17) was eliminated for the computation of the transfer function.

2.3.2. Evaluation based on NDVI values

The sampling strategy is evaluated using the SPOT image by comparing the NDVI distribution over the site with the NDVI distribution over the ESUs (Figure 6). As the number of pixels is drastically different for the ESU and whole site (WS=22500 in case of a 3 x 3 km SPOT image), it is not statistically consistent to directly compare the two NDVI histograms. Therefore, the proposed technique consists in comparing the NDVI cumulative frequency of the two distributions by a Monte-Carlo procedure which aims at comparing the actual frequency to randomly shifted sampling patterns. It consists in:

1. computing the cumulative frequency of the N pixel NDVI that correspond to the exact ESU locations;
2. then, applying a unique random translation to the sampling design (modulo the size of the image);
3. computing the cumulative frequency of NDVI on the randomly shifted sampling design;
4. repeating steps 2 and 3, 199 times with 199 different random translation vectors.

This provides a total population of $N = 199 + 1$(actual) cumulative frequency on which a statistical test at acceptance probability $1 - \alpha = 95\%$ is applied: for a given NDVI level, if the actual ESU density function is between two limits defined by the $N\alpha/2 = 5$ highest and lowest values of the 200 cumulative frequencies, the hypothesis assuming that WS and ESU NDVI distributions are equivalent is accepted, otherwise it is rejected.

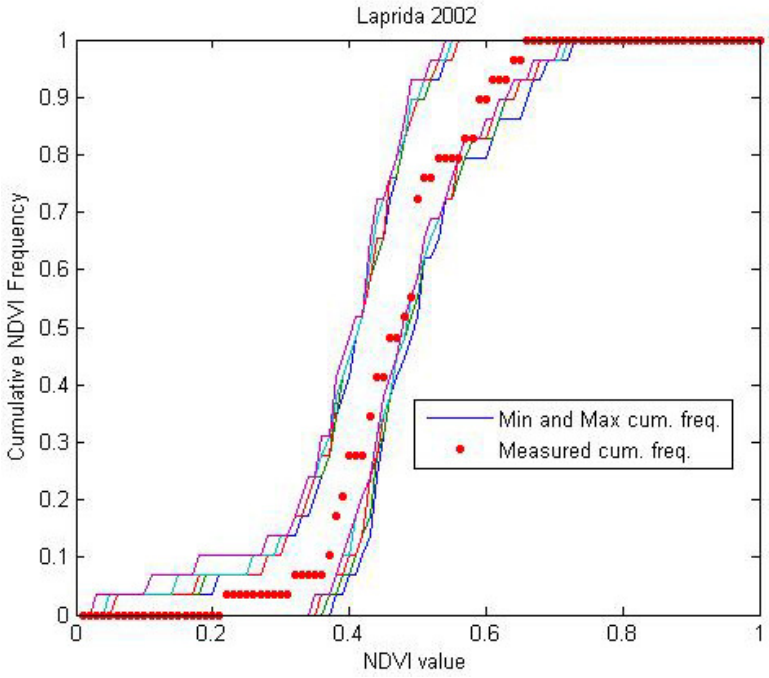

Figure 6. Comparison of the ESU NDVI distribution and the NDVI distribution over the whole image.

Figure 6 shows that the NDVI distribution of the 29 ESUs is very good over the whole site (comprised between the 5 highest and lowest cumulative frequencies) even if the cumulative frequency curve is sometimes close to the boundaries for high NDVI values. It reaches even the boundaries on several occasions since NDVIs have not been sampled between 0.22 and 0.31, 0.33 and 0.37… Note that NDVIs lower than 0.21 have not been sampled either although they are present in the image. They may correspond to roads or paths. Moreover, the site is quite homogeneous in terms of NDVI since the highest and lowest distributions are close.

2.3.3. Evaluation based on classification

A non supervised classification based on the k_means method (Matlab statistics toolbox) was applied to the 4 reflectances of the SPOT image to distinguish if different behaviours on the image for the biophysical variable-reflectance relationship exist.

A number of 5 classes was chosen (Figure 7). The distribution of the classes on the image and on the ESUs is similar. Class 3 is under-represented while classes 1, 2 and 4 appear to be slightly over-sampled.

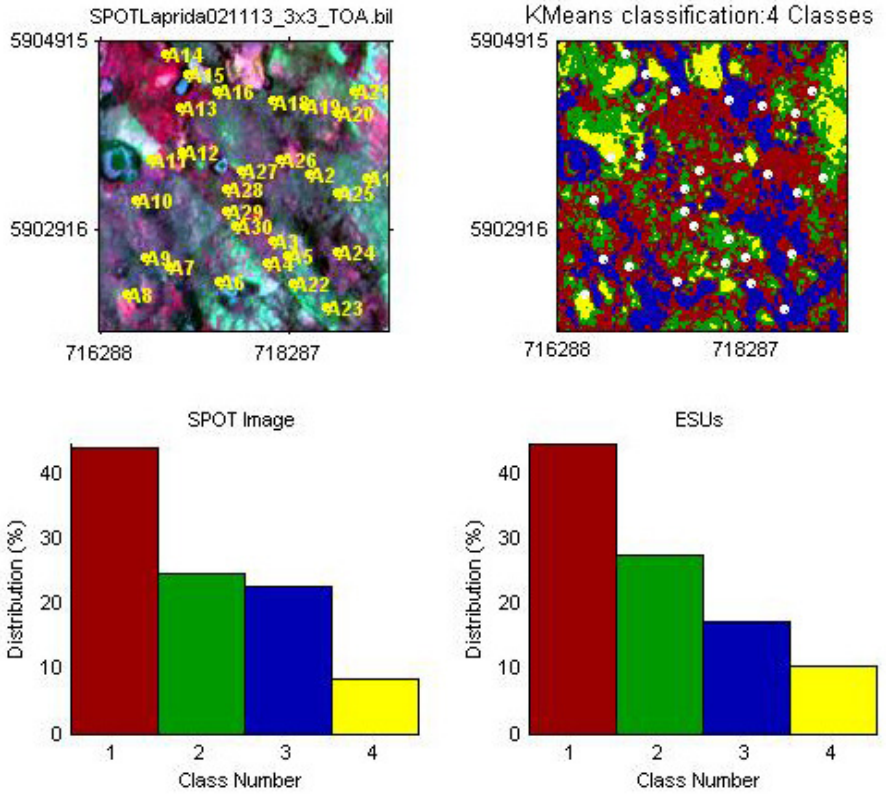

Figure 7. Classification of the SPOT image. Comparison of the class distribution between the SPOT image and sampled ESUs.

Figure 8 shows the different relationships observed between the biophysical variables and the corresponding NDVI on the ESUs, as a function of the SPOT classes determined from non supervised classification.

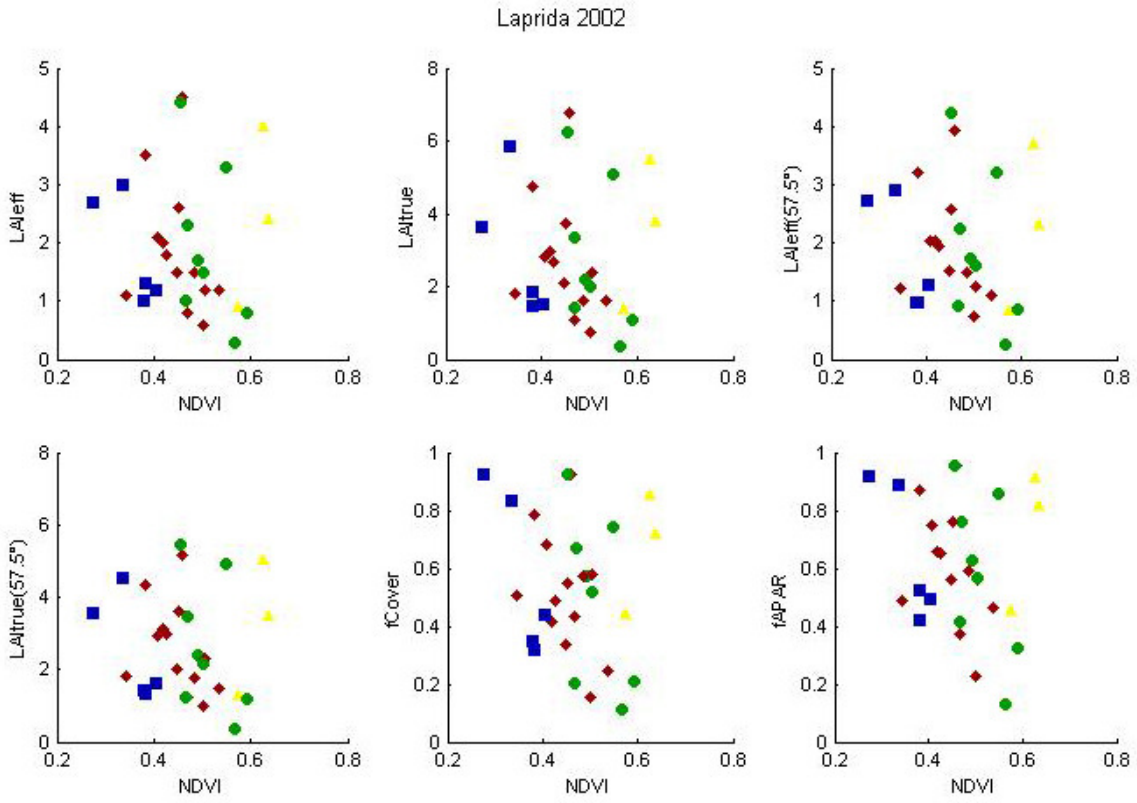

Figure 8. NDVI-Biophysical Variable relationships as a function of SPOT classes

There is no relation between NDVI and biophysical variables although a beer-lamber law was expected. This may be due to two features:

1. a strong presence of water distributed all over the site (the campaign took place few days after floodings in the area) which modify the reflectance signal and therefore the expected LAI-NDVI relationship;

2. the estimation of the biophysical variables (mainly high LAI values) may not be very accurate since it comes to the limits of the hemispherical images + Can-Eye processing: as the LAI is quite high and the images are acquired from above the canopy, it is sometimes very difficult to make the difference between the vegetation and the soil when shadows are observed. This distinction is made worse when the soil is covered by water (water is dark, leaves are quite dark and shadowed leaved are very dark).

2.3.4. Using convex hulls

A test based on the convex hulls was also carried out to characterize the representativeness of ESUs. Whereas the evaluation based on NDVI values uses two bands (red and NIR), this test uses the four bands of the SPOT image. A flag image, is computing over the reflectances (Figure 9). The result on convex-hulls can be interpreted as:

- pixels inside the 'strict convex-hull': a convex-hull is computed using all the SPOT reflectance corresponding to the ESUs belonging to the class. These pixels are well represented by the ground sampling and therefore, when applying a transfer function the degree of confidence in the results will be quite high, since the transfer function will be used as an interpolator;
- pixels inside the 'large convex-hull': a convex-hull is computed using all the reflectance combination (±5% in relative value) corresponding to the ESUs. For these pixels, the degree of confidence in the obtained results will be quite good, since the transfer function is used as an extrapolator (but not far from interpolator);
- pixels outside the two convex-hulls: this means that for these pixels, the transfer function will behave as an extrapolator which makes the results less reliable. However, having a priori information on the site may help to evaluate the extrapolation capacities of the transfer function.

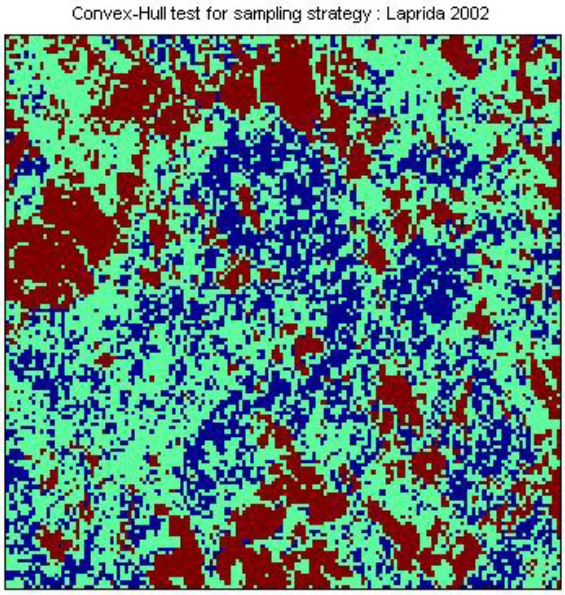

Figure 9. Evaluation of the sampling based on the convex hulls. The map is shown at the bottom: blue and light blue correspond to the pixels belonging to the 'strict' and 'large' convex hulls and red to the pixels for which the transfer function is extrapolating.

This map shows that the representativeness of the ESUs is rather good, even if pixels are outside the two convex-hulls. They correspond to mixed pixels: surface water, elevated area without surface water, pasture… Note that the areas where the NDVI values are high and the surface is covered by water represent the main part of extrapolated pixels. As for the evaluation based on classification, the reflectance signal and the estimation of high LAI values with the software Can-Eye above areas with a strong presence of surface water are in question.

3. Determination of the transfer function for the 6 biophysical variables: LAIeff, LAItrue, LAI57eff, LAI57true, fCover, fAPAR

3.1. The transfer functions considered

Two types of transfer functions are usually tested in the frame of the VALERI project:

- AVE: if the number of ESUs belonging to the class is too low. The transfer function consists only in attributing the average value of the biophysical variable measured on the class to each pixel of the SPOT image belonging to the class;

- REG: if the number of ESUs is sufficient, multiple robust regression between ESUs reflectance (or Simple Ratio) and the considered biophysical variable can be applied: we used the 'robustfit' function from the matlab statistics toolbox. It uses an iteratively re-weighted least squares algorithm, with the weights at each iteration computed by applying the bisquare function to the residuals from the previous iteration. This algorithm provides lower weight to ESUs that do not fit well. The results are less sensitive to outliers in the data as compared with ordinary least squares regression. At the end of the processing, three errors are computed: classical root mean square error (RMSE), weighted RMSE (using the weights attributed to each ESU) and cross-validation RMSE (leave-one-out method).

As there is no evident relationship between NDVI and LAI (§2.3.3), the results of the multiple robust regression (REG) did not show pertinent results. Therefore, even if the number of ESUs belonging to the classes is sufficient, the 'AVE' method is applied. For each class determined in §2.3.3, the transfer function consists only in attributing the average value of the biophysical variable measured on the class to each pixel of the SPOT image belonging to the class.

3.2. Results

Following, the results of the transfer function:

	LAIeff	LAItrue	LAI57eff	LAI57true	fCover	fAPAR
Class 1	1.8769	2.6923	1.8415	2.59	0.51297	0.60796
Class 2	1.9125	2.7212	1.8812	2.6475	0.49325	0.57933
Class 3	1.84	2.866	1.772	2.51	0.5736	0.65019
Class 4	2.4333	3.5433	2.2733	3.2533	0.6694	0.72584

Table 2. Transfer function applied to the whole site for the different biophysical variables

The values of biophysical variable maps are rather homogeneous with close values between classes 1, 2 and 3. On the other hand the class 4 has a specific behaviour. The ESUs[4] (A11, A14) belonging to this class correspond to "elevated area" with or without surface water.

Note that the average value of the ESUs per biophysical variable over the whole Laprida site is also representative of the classes 1, 2 and 3:

	LAIeff.ESU	LAItrue.ESU	LAI57eff.ESU	LAI57true.ESU	fCover.ESU	fAPAR.ESU
Mean	1.937	2.818	1.885	2.660	0.534	0.619

This is not true for class 4.

4. Conclusion

The transfer function is obtained by using 29 ESUs. The Laprida site is heterogeneous in terms of LAI and NDVI. No relationship exists between these two variables (§2.3.3). The representativeness of the ESUs is good even if the transfer function is used as an extrapolator in little areas (§2.3.4). The site is particular since there is a strong presence of surface water. Note that the number and the place of sensor spectral bands do not make it possible to take into account the presence of water correctly. Therefore, the estimation of LAI from the 4 bands

[4] There are no comments about ESU A8 in the campaign report.

is more uncertainly. Moreover the estimation of biophysical variables above grassland with surface water as well as for high LAIs is more difficult with the CAN-EYE software.

Therefore, the selected transfer function consists in attributing the average value of the biophysical variable measured on the class to each pixel of the SPOT image belonging to the class. The average value of the ESUs per biophysical variable over the whole site is also representative of the classes 1, 2 and 3. This is not true for class 4 which is characterized by heterogeneous surfaces.

The biophysical variable maps are available in UTM, 20 South, projection coordinates (Datum: WGS-84) at 20m resolution.

5. Acknowledgements

We thank people who participated to the field experiment: **Mario Carpi** (Farm owner) and **Ricardo Castex** (Farm manager), **Patricio Oricchio** and **Carlos Di Bella** (INTA).

ANNEX

Ground measurement acquisition report for the VALERI site **Laprida**

sampled from 18/10/02 to 19/10/02

Carlos Di Bella
Organization: INTA
email: cdibella@cnia.inta.gov.ar

Date of report 29/10/02

People participating to the field experiment:

Fistname & Name	0rganization
Di Bella, Carlos	INTA
Oricchio, Patricio	INTA
Mario Carpi	Farm owner
Ricardo Castex	Farm manager

Site coordinates

	Lat-Long WGS84 (Deg min.00)		UTM / WGS84 UTM	
	Lat.	Long.	Easting	Northing
Upper left corner	36 58 37.55 S	60 34 12.64 W	716279	5904909
Lower right corner	37 0 12.31 S	60 32 8.27 W	719279	5901909

Ground control points

*This is extracted from the Excel file GPSSIteNameYear.xls

GCP1	722127	5902721	50 mts la Cartila entry
GCP2	722226	5902763	La Cartila entry
GCP3	725505	5903826	Road with Rail
GCP4	728442	5904999	Road cross
GCP5	728736	5905188	Road with rail
GCP6	734491	5911459	Road cross

Description of the site and land cover

Category according to IGBP classification

Grasslands.

Comments on the land cover

Native and successional grasslands in both Flooding and Southern Pampa are characterised by the co-dominance of C3 and C4 grasses. Aboveground net primary 127 production of these grasslands range between 4500 and 5500 kg m -2 y -1. The climate is humid temperate, with a mean annual precipitation 129 between 700 and 800 mm y -1 and mean annual temperature of 14°C. Perennial pastures, used for cattle grazing of hay production, are very extensive in the area. They are often composed by alfalfa alone or alfalfa plus some C3 grass like Bromus unioloides or Dactylis glomerata. Pastures are generally part of the crop rotation system. They are used during 3 to 6 years and then the paddock is used for annual crops again. Where soil conditions are not appropriate for cropping, it is frequent that native grasslands are inter-sowed with Agropyron sp. or Festuca arundinacea[5].

Topography

Altitude ≈ 200m.

[5] Guerschman, JP; Paruelo, JM; Di Bella, CM; Giallorenzi, MC and Pacin, F (2001): Land Cover Classification in Argentine Pampas using multitemporal landsat TM data. **International Journal of Remote Sensing (Accepted)**.

Land cover map

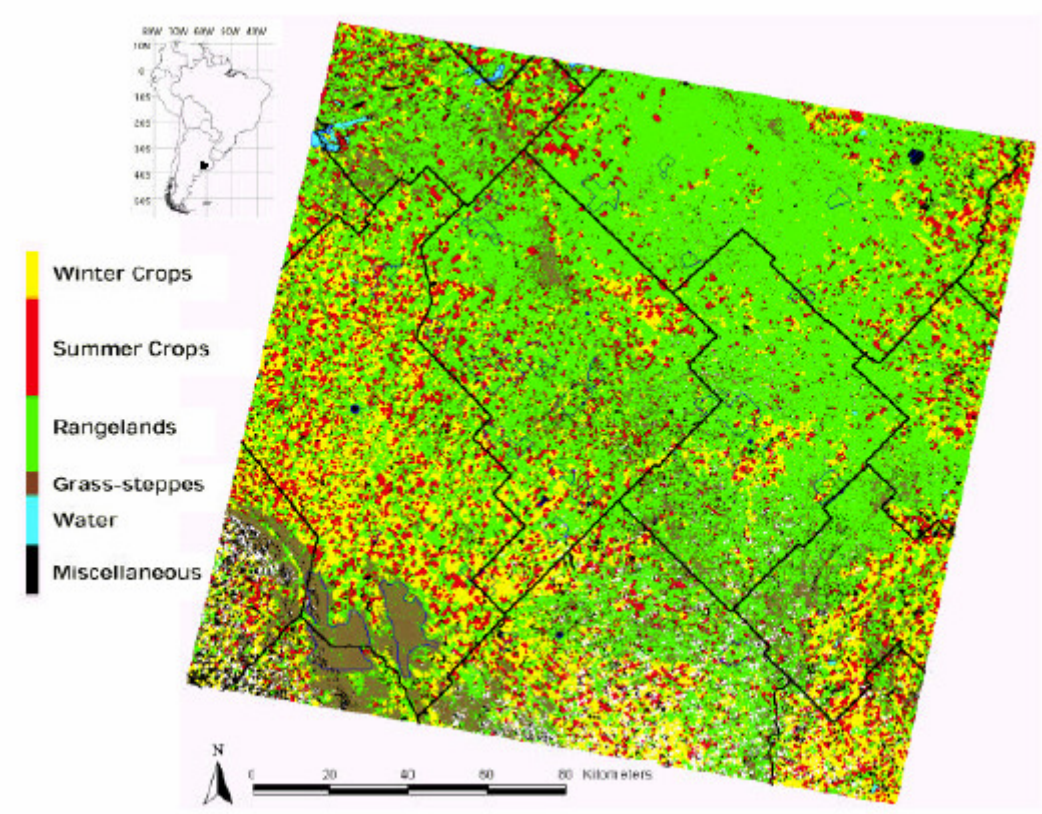

Spatial Sampling scheme

Sensors used for sampling the ESUs

	Method	Comments
☒	Hemispherical photographs	
☐	LAI2000	
☐	TRAC	
☐	Ceptometer	
☐	Direct measurements	
☐	Other	

Sampling strategy for the ESU

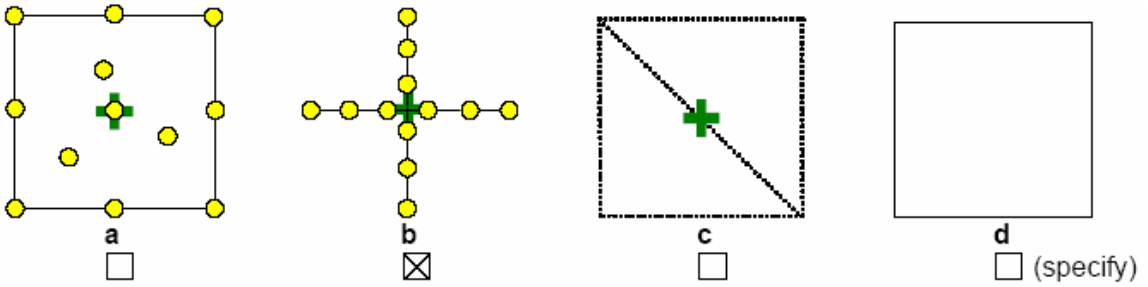

Distribution of the Elementary sampling units

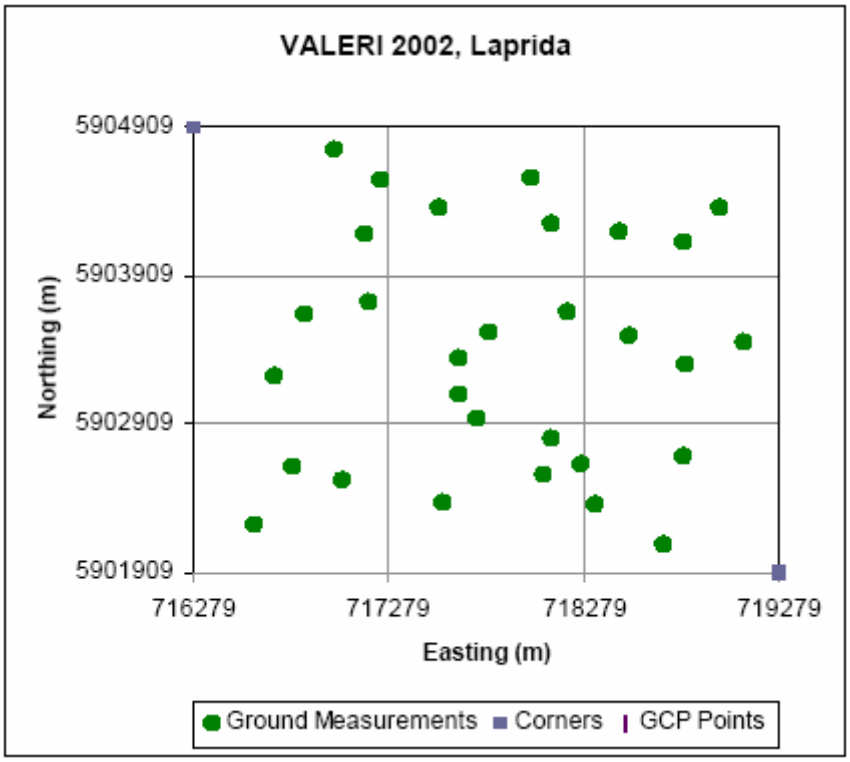

The high spatial resolution image

Satellite

Satellite used	Sensor
Level of processing	Choose a level
Projection type	

List of the ESUs

A1	719095	5903464	
A2	718504	5903502	
A3	718108	5902813	
A4	718065	5902573	
A5	718263	5902643	
A6	717553	5902383	At one sido of a lagune
A7	717040	5902529	
A8	716585	5902240	
A9	716778	5902623	Natural grassland with water and stand dead biomass
A10	716689	5903235	Some water and high canopy
A11	716841	5903652	Cyperus (typical of permanent water) at one side of an elevated area (cardus)
A12	717173	5903730	Cutted biomass, high stocking density and intermediate water
A13	717157	5904193	Water, 50 mts lagune with cattle
A14	716999	5904763	Elevated area without water and high animal density
A15	717233	5904551	Pasture without water, cattle, one side of a lagune
A16	717534	5904367	Cyperus in floration, little water
A17	718003	5904570	Elevated area without water, without cattle
A18	718111	5904267	Flooded area, cyperus
A19	718454	5904211	Cattle, little water
A20	718789	5904134	Elevated land, no water, with cattle
A21	718966	5904369	Cutted biomass, floration POA
A22	718331	5902363	Pasture, no cattle, the dream area
A23	718686	5902102	Low vegetation density, a little flooded
A24	718790	5902695	Festuca, pasture, little water, torus area
A25	718799	5903316	Elevated land, without water, feedlot area
A26	718186	5903666	The highest water measured level
A27	717791	5903533	
A28	717633	5903353	
A29	717638	5903106	
A30	717729	5902956	

This is extracted from the Excel file GPSLaprida2002.xls

Acknowledgements

We want to thank Mr. Mario Carpi and Ricardo Castex (owner and manager of the farm, respectively) for the invaluable help in the measurements.

Photo gallery

The photos illustrating the campaign are to be stored in the directory “photo gallery” and the labels should be indicated in the table above:

#	File name	Comments
1	A1	Corresponding to the First point (A!) marker
2		
3		
4		
5		
6		
7		
8		
9		
10		
11		
12		
13		
14		
15		
16		
17		
18		
19		
20		
21		
22		
23		
24		
25		
26		
27		
28		
29		
30	A30	Corresponding to the First point (A30) marker